

Article

On the Application of Thévenin Equivalent Circuits to the Analysis of Vacuum Tube Circuits

Aaron Lanterman 

School of Electrical and Computer Engineering, Georgia Institute of Technology, 777 Atlantic Drive, Atlanta, GA 30332, USA; lanterma@ece.gatech.edu

Abstract: In this paper, we express Thévenin equivalent circuits seen looking into the terminals of the small-signal model of the vacuum tube triode in terms of the Thévenin equivalent circuits seen looking out of the other terminals and apply them to the analysis of the common-cathode, common-plate, and common-grid single-tube amplifier configurations, as well as a differential pair amplifier. This is an adaptation of equivalent circuit techniques for transistor circuits pioneered by Marshall Leach. The use of equivalent circuits can yield intuitive solutions that avoid solving sets of equations.

Keywords: equivalent circuits; vacuum tubes; triodes; valves; guitar amplifiers

1. Introduction

Although vacuum tubes gave way to transistors during the 1960s and 1970s, they retain a niche status in audio applications [1–8], where they are particularly favored by electric guitarists [9–19] and audiophiles [20–24].

The creation of Thévenin and Norton equivalent circuits is a powerful technique, finding applications in electronics [25] and power systems [26–31], particularly battery modeling [32–34].

In 1996, Marshall Leach, a professor at the Georgia Institute of Technology, published a paper [35] titled “On the Application of Thévenin and Norton Equivalent Circuits and Signal Flow Graphs to the Analysis of Active Circuits”. In that work, he formulated a Norton equivalent circuit looking into the collector of a bipolar junction transistor (BJT) in terms of the Thévenin equivalents seen looking out of the base and the emitter, a Thévenin equivalent circuit looking into the emitter in terms of the Thévenin equivalent seen looking out of the base, and a Thévenin equivalent circuit looking into the base in terms of the Thévenin equivalent seen looking out of the emitter. Similarly, he formulated a Norton equivalent circuit looking into the drain of a field-effect transistor (FET) in terms of the Thévenin equivalents seen looking out of the gate and the source and a Thévenin equivalent looking into the source in terms of the Thévenin equivalent seen looking out of the gate.

Until he passed away in November 2010, Prof. Leach taught ECE3050: Analog Electronics at Georgia Tech using these equivalent circuits, along with extensive use of superposition with dependent sources. (To this day, most introductory circuits textbooks incorrectly insist that dependent sources may not be “deactivated” when using superposition. The key is to include all contributions before solving for the controlling variable. Numerous examples are provided in [36]; see [37] for technical details. The technique appears to have been independently discovered by Davis [38], who refers to it using the terminology of “taping” and “untaping”.) Prof. Leach introduced the hybrid- π (see pp. 799–805 and pp. 819–821 of [39] or pp. 385–387 and pp. 405–406 of [40]) and T (see p. 849 of [39] or pp. 393–394 and pp. 405–406 of [40]) small-signal models for BJTs and FETs but stuck with them only long enough to derive his Thévenin and Norton equivalent circuits, which he used throughout the semester to derive the typical results of a junior analog electronics



Citation: Lanterman, A. On the Application of Thévenin Equivalent Circuits to the Analysis of Vacuum Tube Circuits. *Electronics* **2023**, *12*, 4804. <https://doi.org/10.3390/electronics12234804>

Received: 12 November 2023
Revised: 25 November 2023
Accepted: 26 November 2023
Published: 27 November 2023



Copyright: © 2023 by the authors. Licensee MDPI, Basel, Switzerland. This article is an open access article distributed under the terms and conditions of the Creative Commons Attribution (CC BY) license (<https://creativecommons.org/licenses/by/4.0/>).

course, without making explicit reference to the underlying small-signal models. Reading a typical electronics textbook, different patterns repeatedly emerge that the equivalent circuits abstract in the way a computer programmer may notice certain repeated patterns in their code and abstract those using a subroutine. He also employed these techniques while teaching the graduate class ECE6416: Low-Noise Electronic Design (see Section 7.7 of [41]). Websites for Marshall Leach’s classes, including ECE3050 and ECE6416, are archived at <https://leachlegacy.ece.gatech.edu> (last accessed on 25 November 2023).

In 2017, the author taught the first offering of a special-topics class titled “Guitar Amplification and Effects”, which largely focused on vacuum tube circuits, in which he made repeated use of the classic voltage-controlled voltage source (VCVS) small-signal model for a triode. The author discovered Prof. Leach’s approach to teaching electronics in 2018 when he first taught the junior Analog Electronics course and found it to be particularly elegant, allowing some results to flow naturally, almost “by inspection”. Therefore, in 2019, during the second offering of “Guitar Amplification and Effects”, he adapted Prof. Leach’s equivalent-circuit-based techniques to vacuum tubes. This paper presents the resulting equivalent circuits, which have not appeared before in the literature, and some of their applications. It also partially serves as an introduction to vacuum tube circuits for practitioners already accustomed to transistors. Much wisdom about tubes is found in texts [42–44] that are over seven decades old; the way schematics are drawn, the terminology used, and even the conceptualization of circuits in these works can seem quite alien to a modern electrical engineer.

2. Thévenin Equivalent Circuits

The leftmost circuit in Figure 1 represents a triode in a generic small-signal circuit. Small-signal quantities v_{tg} and v_{tk} represent the Thévenin voltages seen looking out of the grid and cathode, respectively. R_{tp} and R_{tk} represent the Thévenin resistances seen looking out of the plate and cathode, respectively. Under normal operation, no current flows through the grid, so our analysis does not require knowledge of the resistance seen looking out of the grid, so it is omitted from the diagram, but one could add R_{tg} to the diagram if desired. We use lowercase letters to represent dynamic resistances arising from small-signal models. The use of upper case for R_{tp} and R_{tk} assumes fixed resistances; in the case of a more complex circuit, these may also be dynamic quantities, in which case symbols like r_{tp} and/or r_{tk} might be more appropriate.

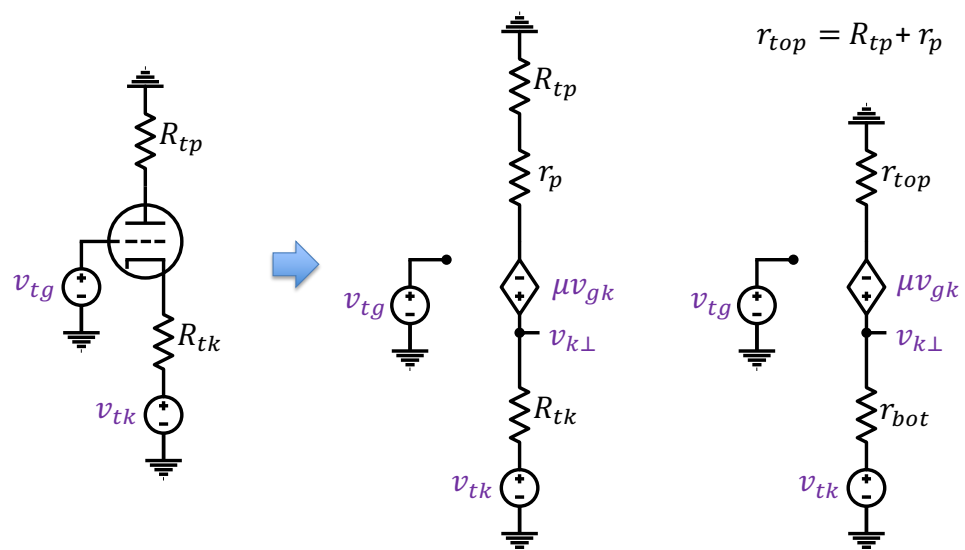


Figure 1. Small-signal triode model with Thévenin equivalents seen looking out of the plate, grid, and cathode (left), explicitly expanded into the VCVS (μv_{gk}) in series with the dynamic plate resistance (r_p) (middle). In the diagram on the right, R_{tp} and r_p are combined into r_{top} .

The arrow in Figure 1 indicates the expansion of the triode into its small-signal model, which consists of a voltage-controlled voltage source (VCVS) with an intrinsic amplification factor (μ) in series with the dynamic plate resistance (r_p). This is analogous to the hybrid- π model for transistors. Note that the negative terminal of the VCVS is on top. The voltage of the VCVS is μv_{gk} , where v_{gk} is the difference between the voltage at the gate (which is just v_{tg}) and the voltage at the cathode, as denoted by $v_{k\perp}$ (where \perp indicates the voltage at the cathode with respect to ground), so $v_{gk} = v_{tg} - v_{k\perp}$.

Small-signal parameters μ and r_p (pp. 16–23 of [45]) depend on the plate bias current, which is typically derived from a load-line analysis (see pp. 55–60 of [46], pp. 7–9 of [47], pp. 33–37 of [48], and pp. 191–195 of [49] for examples). Although r_p notably varies with bias current, μ is usually constant over a wide range of currents. Compared with parameters such as the transconductance of a transistor, which can vary wildly under different operating conditions and between different specimens of the same transistor model, μ is a parameter a designer can rely upon.

For convenience, we define $r_{top} = R_{tp} + r_p$, and for consistency, we define $r_{bot} = R_K$, as shown in the rightmost diagram in Figure 1. We find it illuminating to consider a Thévenin equivalent circuit found looking into the negative terminal of the VCVS and not the top of r_p ; hence, although we find equivalent circuits looking into the cathode, we do not strictly find equivalent circuits looking into the plate. We imagine that we can access an “inner plate” between r_p and the VCVS; this shortens the description of the Thévenin equivalent, but one needs to remember to add r_p .

2.1. Looking into the “Inner Plate”

Given v_{down} , the Thévenin voltage seen looking down into the negative terminal of the VCVS in Figure 2 is an open-circuit voltage; no current flows through the circuit, and therefore, no voltage is lost over r_{bot} . Thus,

$$v_{down} = v_{tk} - \mu(v_{tg} - v_{tk}) = (\mu + 1)v_{tk} - \mu v_{tg}. \tag{1}$$

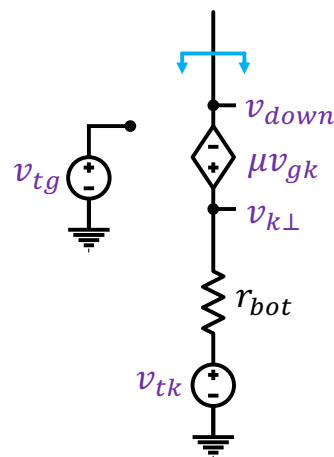


Figure 2. Circuit for the computation of the Thévenin voltage seen looking down into the negative terminal of the VCVS of the small-signal triode model.

To compute the equivalent resistance seen looking down into the negative terminal of the VCVS, we zero the independent sources (v_{tg} and v_{tk}); introduce an independent test current source (i_{test}), as shown in Figure 3; and compute the resulting v_{test} . Since $v_{k\perp} = i_{test}r_{bot}$,

$$v_{test} = v_{k\perp} - \mu(-v_{k\perp}) = (\mu + 1)v_{k\perp} = (\mu + 1)i_{test}r_{bot}. \tag{2}$$

Hence, the equivalent resistance is

$$r_{down} = \frac{v_{test}}{i_{test}} = (\mu + 1)r_{bot}. \tag{3}$$

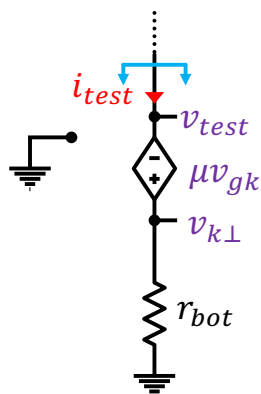


Figure 3. Circuit for computing the equivalent resistance seen looking down into the negative terminal of the VCVS of the small-signal triode model.

Figure 4 summarizes the resulting Thévenin equivalent circuit.

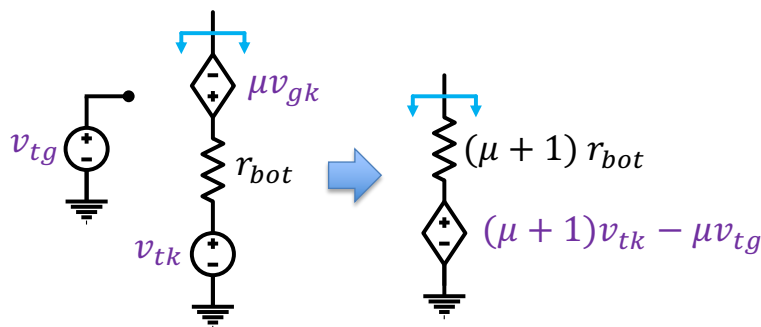


Figure 4. Summary of the Thévenin equivalent circuit seen looking down into the negative terminal of the VCVS of the small-signal triode model. We repeatedly refer to this figure in this paper.

2.2. Looking into the Cathode

Since v_{up} , the Thévenin voltage seen looking up into the positive terminal of the VCVS in Figure 5 is an open-circuit voltage; no current flows through the circuit, and therefore, no voltage is lost over r_{top} . Thus,

$$v_{up} = \mu(v_{tg} - v_{up}), \tag{4}$$

$$v_{up} = \frac{\mu}{\mu + 1}v_{tg}. \tag{5}$$

To compute the equivalent resistance seen looking up into the positive terminal of the VCVS, we zero the independent source (v_{tg}); introduce an independent test voltage source (v_{test}), as shown in Figure 6; and compute the resulting i_{test} . Since $\mu v_{gk} = -\mu v_{test}$, we can compute the voltage at the negative terminal of the VCVS as $\mu v_{test} + v_{test} = (\mu + 1)v_{test}$. Hence,

$$i_{test} = \frac{(\mu + 1)v_{test}}{r_{top}}. \tag{6}$$

The equivalent resistance is

$$r_{up} = \frac{v_{test}}{i_{test}} = \frac{r_{top}}{\mu + 1}. \tag{7}$$

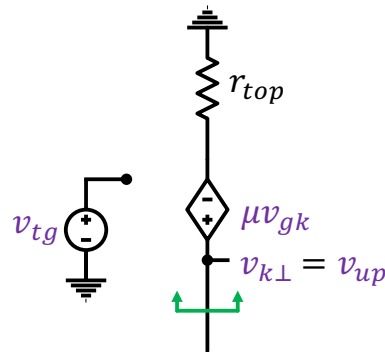


Figure 5. Circuit for computing the Thévenin voltage seen looking up into the positive terminal of the VCVS of the small-signal triode model.

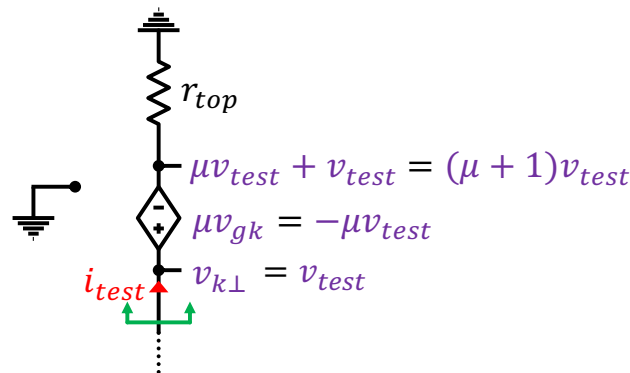


Figure 6. Circuit for computing the equivalent resistance seen looking up into the positive terminal of the VCVS of the small-signal triode model.

Figure 7 summarizes the resulting Thévenin equivalent circuit.

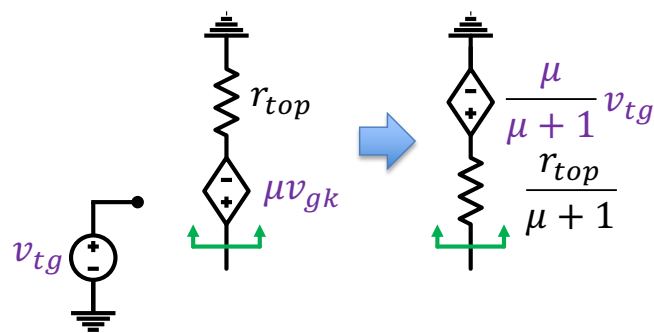


Figure 7. Summary of the Thévenin equivalent circuit seen looking up into the positive terminal of the VCVS of the small-signal triode model. We repeatedly refer to this figure in this paper.

3. Applications

Throughout this section, small-signal circuit quantities are represented using lowercase variables with lowercase subscripts, DC bias quantities are represented using uppercase variables with uppercase subscripts, and total quantities are represented using lowercase variables with uppercase subscripts, such as $v_{OUT} = V_{OUT} + v_{out}$.

In this paper, capacitors are assumed to act as short circuits at audio frequencies. The methods described here can be extended to frequency analyses using the methods of short-circuit and open-circuit time constants.

3.1. Common-Cathode Amplifier

The left diagram in Figure 8 shows a typical self-biased common-cathode amplifier (based on Figure 5.7 of [50]). The input at the grid is ground-referenced via the grid leak resistor (R_G), so $v_{in} = v_{IN}$. R_{KG} denotes a resistor connecting the cathode to ground, and R_{KC} denotes a resistor connecting the cathode to the capacitor (C_K). We refer to the plate resistor as R_L instead of R_P to avoid confusion with the notation for the dynamic small-signal plate resistance (r_p). “L” in this context stands for “load”, but this should be thought of as part of the amplifier and not as representing an external load.

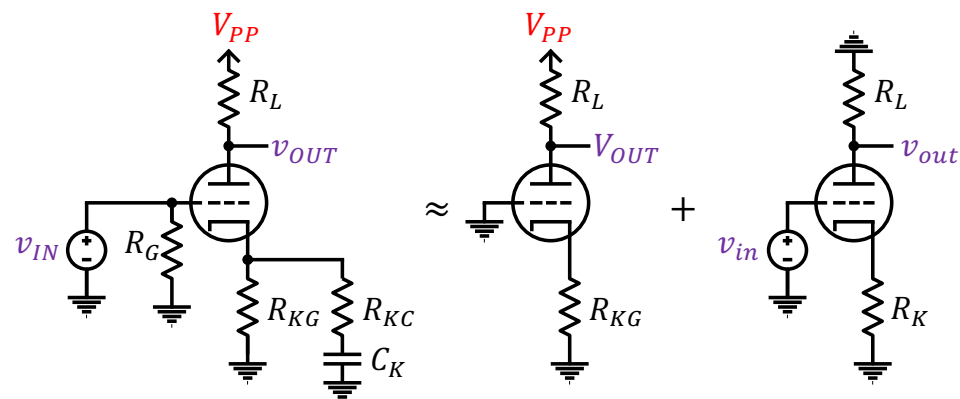


Figure 8. A typical self-biased common-cathode amplifier decomposed into its DC bias and small-signal circuits. Many authors rearrange small-signal circuits so that “ac” grounds point downward along with “real” grounds. Although this typically results in more compact schematics, we have found it helpful to leave the original arrangement in place to help visualize how aspects of the small-signal circuit relate to the original full circuit.

The diagrams to the right of the approximation sign in Figure 8 illustrate decomposition into DC bias (middle) and small-signal (right) circuits, where $R_K = R_{KG} \parallel R_{KC}$. At DC, the capacitor is an open circuit, so R_{KC} plays no role in the biasing. In the special case of $R_{KC} = 0$, R_{KG} is completely bypassed, and we have no “cathode degeneration” (see pp. 267–290 of [51] for examples).

The left diagram in Figure 9 shows the underlying small-signal model replacing the triode symbol in the right diagram of Figure 8. This forms the basis of the usual analysis of the amplifier, as may be found on pp. 39–41 of [52]. Skipping the small-signal model and applying the Thévenin equivalent in Figure 4 yields the right diagram of Figure 9, which permits a more direct solution via voltage division:

$$v_{out} = -v_{in} \mu \frac{R_L}{R_L + r_p + (\mu + 1)R_K}. \tag{8}$$

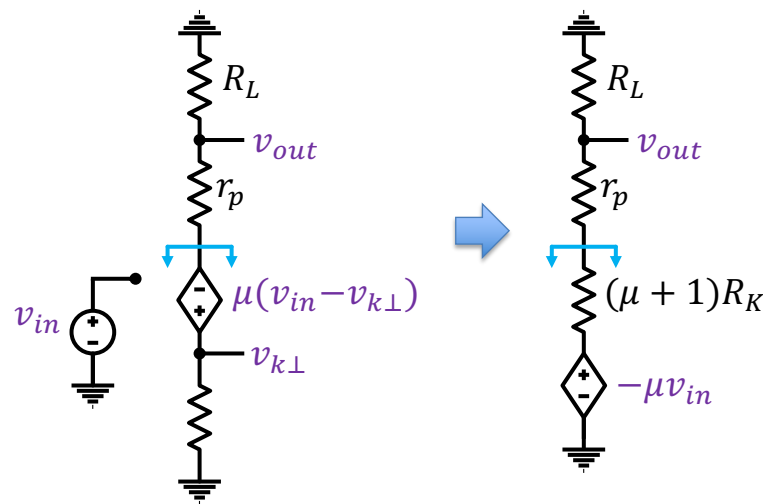


Figure 9. The left diagram shows the right diagram of Figure 8 with the small-signal triode model explicitly expanded. In the right diagram, the portions of the circuit looking into the negative terminal of the VCVS of the small-signal model are replaced with the associated Thévenin equivalent.

Zeroing the input source yields the output impedance:

$$r_{out} = R_L \parallel [r_p + (\mu + 1)R_K]. \tag{9}$$

In the completely bypassed case, where $R_K = 0$, we have $v_{out} = -v_{in}\mu R_L / (R_L + r_p)$ and $r_{out} = R_L \parallel r_p$.

Since no current flows through the grid, the input impedance is set by R_G , which is typically a large value (in the range of megaohms).

3.2. Common-Plate Amplifier (Cathode Follower)

The left diagram of Figure 10 shows a typical common-plate amplifier, also known as a cathode follower. The flexibility of R'_K and R_T allows for more practical biasing than if the grid leak resistor (R_G) was hooked to ground, as in the previous example of the common-cathode amplifier. Some practitioners prefer to take the output from the junction of R'_K and R_T (labeled V_{OUT}^{alt}) instead of the directly from the cathode (labeled V_{OUT}). We omitted the DC blocking capacitors typically present at the output.

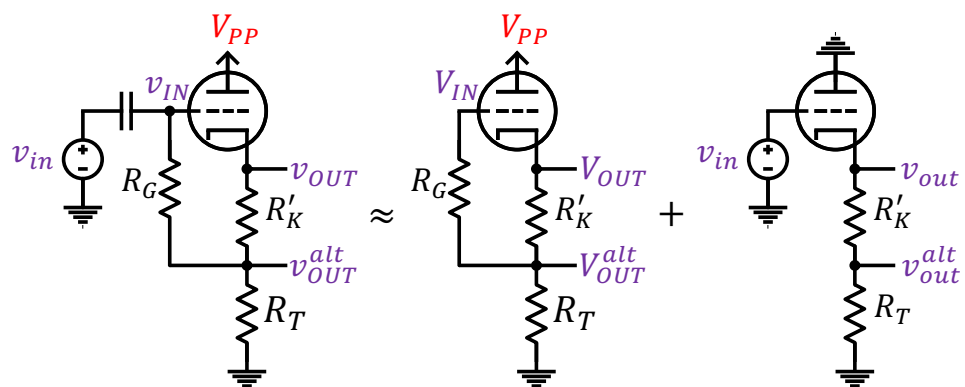


Figure 10. Typical self-biased voltage follower decomposed into its DC bias and small-signal circuits.

The two rightmost diagrams of Figure 10 illustrate decomposition into DC bias (middle) and small-signal (right) circuits, assuming that R_G is large enough that it can be neglected in the small-signal analysis.

Invoking the Thévenin equivalent circuit in Figure 7 (with $r_{top} = r_p$), we can immediately find the outputs via voltage division:

$$v_{out} = v_{in} \frac{\mu}{\mu + 1} \cdot \frac{R'_K + R_T}{R'_K + R_T + \frac{r_p}{\mu + 1}} = v_{in} \frac{\mu(R'_K + R_T)}{(\mu + 1)(R'_K + R_T) + r_p}, \tag{10}$$

$$v_{out}^{alt} = v_{in} \frac{\mu}{\mu + 1} \cdot \frac{R_T}{R'_K + R_T + \frac{r_p}{\mu + 1}} = v_{in} \frac{\mu R_T}{(\mu + 1)(R'_K + R_T) + r_p}. \tag{11}$$

As μ increases, v_{out} approaches v_{in} , and v_{out}^{alt} approaches $v_{in} R_T / (R'_K + R_T)$, justifying the name “cathode follower.”

Zeroing the input source yields the following output impedances:

$$r_{out} = (R'_K + R_T) \parallel \frac{r_p}{\mu + 1}, \tag{12}$$

$$r_{out}^{alt} = R_T \parallel \left(R'_K + \frac{r_p}{\mu + 1} \right). \tag{13}$$

Note that the output impedance improves as μ increases.

The input impedance of this particular configuration is even better than that of the common-cathode amplifier due to a “bootstrapping” effect. Since v_{out}^{alt} is only slightly less than v_{in} , if we reintroduce R_G to the small-signal circuit, we see that very little current flows across it relative to an R_G hooked between v_{in} and ground. We do not address this in further detail here; we mention it to contrast with the input impedance of the common-grid amplifier discussed in the next section.

3.3. Common-Grid Amplifier

The left diagram of Figure 11 shows a typical common-grid amplifier (also known as a “grounded grid” amplifier). Such amplifiers have a niche application in high-frequency amplifiers (see pp. 395–397 of [53] and p. 195 of [54]) but are not very common in audio amplifiers; however, they are helpful as building blocks in terms of understanding more complex amplifier structures such as cascodes and differential pair amplifiers, which are addressed in Section 3.4.

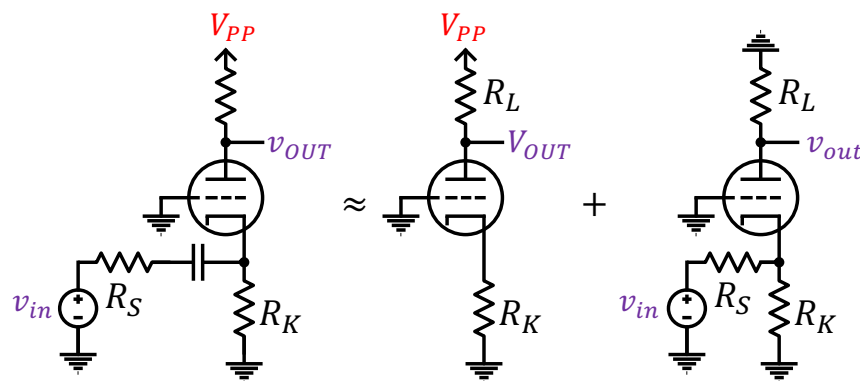


Figure 11. Typical common-grid amplifier with a source impedance.

In Figure 11, R_S represents the output impedance of the source driving the amplifier and is not part of the amplifier itself. We include it here because it appears in the expression for the amplifier’s output impedance, which is not the case for any source impedances for the common-cathode and common-plate configurations.

The two rightmost diagrams of Figure 10 show the amplifier’s decomposition into DC bias (middle) and small-signal (right) circuits. To find the output voltage and output impedance, we want to find the Thévenin equivalent circuit seen looking into the plate; but to find that, we first need the Thévenin equivalent circuit seen looking out of the cathode.

As illustrated in Figure 12, the equivalent resistance is just R_K in parallel with R_S , and the Thévenin voltage is found via a voltage divider, yielding $v_{in}R_K/(R_S + R_K)$.

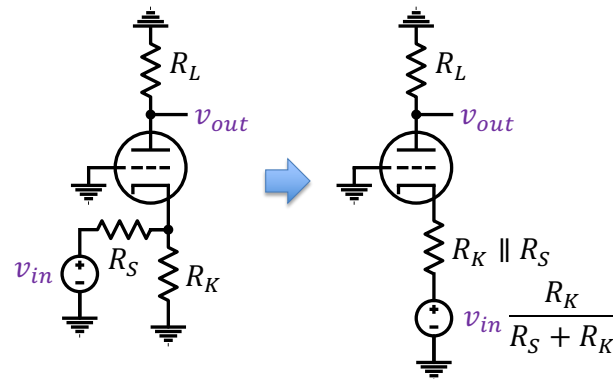


Figure 12. The common-grid small-signal model shown in the right diagram of Figure 11 is repeated on the left here. This figure illustrates the replacement of the components seen looking out of the cathode with a Thévenin equivalent circuit.

We can now find the Thévenin equivalent circuit seen looking into the plate, as visualized in Figure 13. According to Figure 4, the resistance ($r_{bot} = R_K || R_S$) when seen from the other side tube appears as $(\mu + 1)(R_K || R_S)$, which is in series with the dynamic plate resistance (r_p). Similarly, the voltage ($v_{in}R_K/(R_S + R_K)$) is multiplied by $(\mu + 1)$.

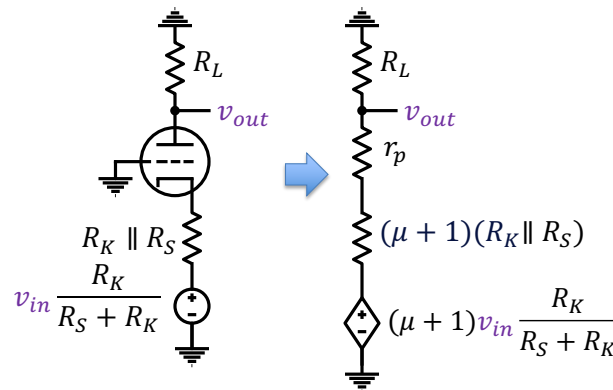


Figure 13. The right diagram of Figure 12 is repeated on the left here. This figure illustrates the use of the Thévenin equivalent circuit seen looking into the plate in order to find the voltage gain and the output impedance.

Voltage division yields the output voltage:

$$v_{out} = v_{in} \frac{(\mu + 1)R_K}{R_S + R_K} \cdot \frac{R_L}{R_L + r_p + (\mu + 1)(R_K || R_S)}. \tag{14}$$

Zeroing the input yields the output impedance:

$$r_{out} = R_L || [r_p + (\mu + 1)(R_K || R_S)]. \tag{15}$$

Finally, we calculate the input impedance seen looking from the right side of R_S into the junction of R_K and the cathode in the small-signal circuit (right diagram of Figure 11). For this, we need the Thévenin equivalent circuit looking up into the cathode; applying Figure 7 yields the right diagram of Figure 14, from which we find

$$r_{in} = R_K || \left(\frac{R_L + r_p}{\mu + 1} \right). \tag{16}$$

This explains why common-grid amplifiers are not as common as common-cathode amplifiers; their input impedance (assuming information is represented as a voltage) is poor in comparison and becomes worse as μ increases.

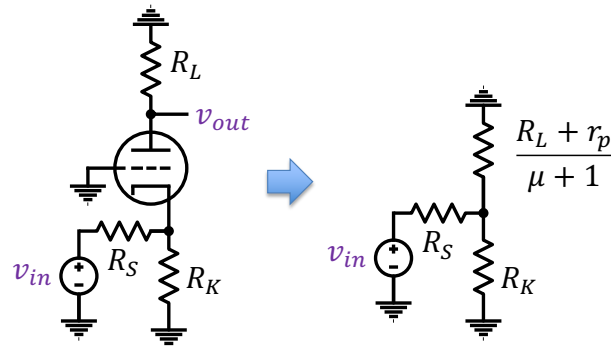


Figure 14. The common-grid small-signal model shown in the right diagram of Figure 11 is repeated on the left here. This figure illustrates the use of a Thévenin equivalent circuit seen looking up into the cathode to find an input impedance.

3.4. Differential Amplifier: The Long-Tailed Pair

Transistor-based audio amplifiers often have a push-pull output stage consisting of a complementary pair, such as an NPN and a PNP or an nFET and a pFET. Vacuum tubes are somewhat analogous to NPNs or nFETs; there is no tube equivalent of a PNP or pFET. Hence, building a push-pull stage with vacuum tubes is like having to build a push-pull stage with only NPNs or only nFETs. Hence, a “phase splitter” is needed to create an inverted copy of the original signal [55]. One approach is to simply use an inverting unity-gain common-cathode amplifier while leaving the original signal alone; this is referred to as a “paraphase inverter”. Another approach, referred to as a “cathodyne” or “concertina”, is to add a plate resistor to a cathode follower as in Section 3.2, forming a combination of a cathode follower and a common-cathode amplifier, which provides buffering for the original signal. This can be analyzed by adding a fixed plate load resistance (R_L) to the dynamic plate resistance (r_p) in the formulas presented in Section 3.2.

A third approach is to use a differential amplifier such as that shown in in Figure 15, colloquially known as a “long-tailed pair”, which has the advantage of offering gain in addition to providing original and inverted signals. Letting $R_K = R'_K + R_T$, Figure 16 shows the corresponding small-signal circuit, assuming that grid leak resistances (R_G) are sufficiently large that they can be neglected in the small-signal analysis.

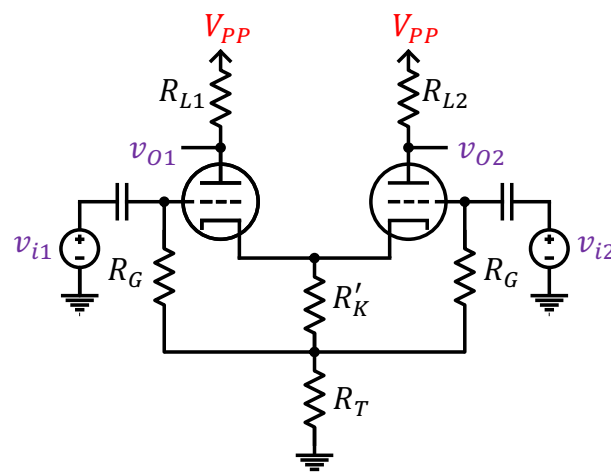


Figure 15. Typical self-biased differential amplifier.

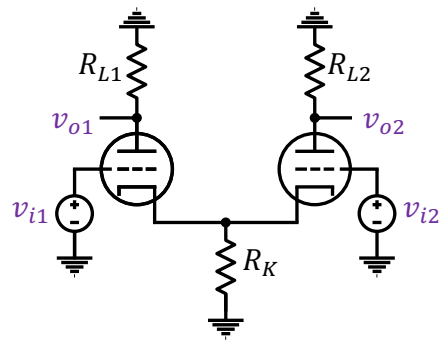


Figure 16. Small-signal circuit for the differential amplifier in Figure 15, with $R_K = R'_K + R_T$.

This exposition focuses on v_{o1} ; the results for v_{o2} can be found by swapping variables. We tackle the circuit via superposition, zeroing v_{i2} , and by considering the effect of v_{i1} , then by zeroing v_{i1} and considering the effect of v_{i2} , which is a slightly more complicated situation.

We begin by studying the effect of v_{i1} in v_{o1} . As illustrated in Figure 17, if we zero v_{i2} , we can replace the right tube and R_{L2} with r_{ki2} , the Thévenin equivalent resistance seen looking into the cathode of the right tube:

$$r_{ki2} = \frac{r_p + R_{L2}}{\mu + 1}. \tag{17}$$

Combining the parallel resistances (R_K and r_{ki2}), Figure 18 clarifies that we have the form of a common-cathode amplifier. Applying (8) yields

$$v_{o1} = -v_{i1} \frac{\mu R_{L1}}{R_{L1} + r_p + (\mu + 1)(R_K \parallel r_{ki2})}. \tag{18}$$

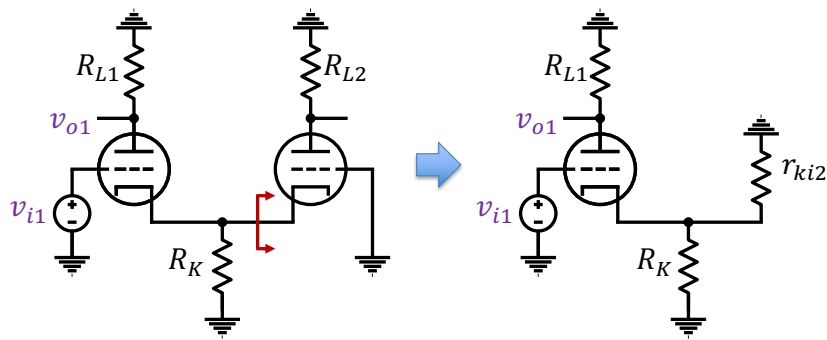


Figure 17. Letting $v_{i2} = 0$ in Figure 16 and replacing the portion of the small-signal circuit looking into the cathode of the right tube with its equivalent resistance.

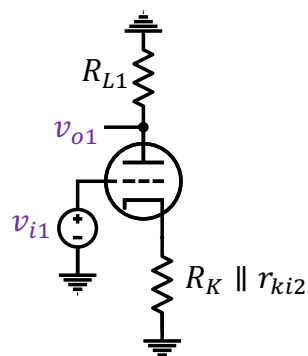


Figure 18. The parallel combination of R_K and r_{ki2} in Figure 17.

We now zero v_{i1} and study the effect of v_{i2} on v_{o1} . As illustrated in Figure 19, if we zero v_{i2} , we can replace the right tube and R_{L2} with the Thévenin equivalent circuit looking into the cathode of the right tube according to Figure 7.

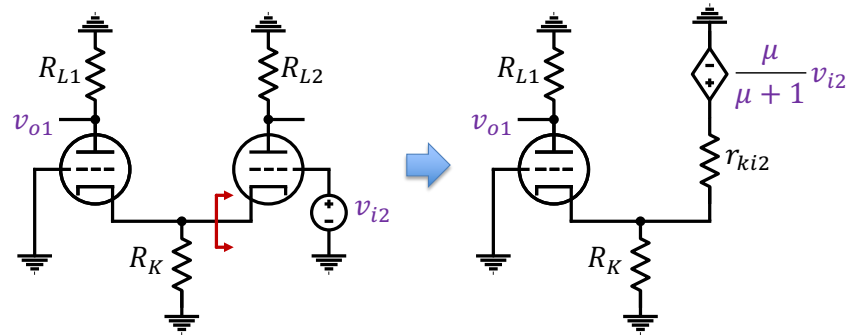


Figure 19. Letting $v_{i1} = 0$ in Figure 16 and replacing the portion of the small-signal circuit looking into the cathode of the right tube with its Thévenin equivalent.

We can then find a Thévenin equivalent circuit looking out of the cathode of the left tube, as shown in Figure 20. The Thévenin voltage can be found with a voltage divider, and the Thévenin resistance is just a parallel combination. The circuit now resembles a common-grid amplifier. Employing the Thévenin equivalent of Figure 4 reveals Figure 21, in which the $\mu + 1$ factors in the numerator and the denominator of the multiplier of the VCVS cancel each other out. We can then find v_{o1} via voltage division:

$$v_{o1} = v_{i2} \frac{\mu R_{L1}}{R_{L1} + r_p + (\mu + 1)(R_K \parallel r_{ki2})} \cdot \frac{R_K}{R_K + r_{ki2}}. \tag{19}$$

Note that (19) resembles (18), with v_{i2} replacing v_{i1} , multiplied by $-R_K / (R_K + r_{ki2})$.

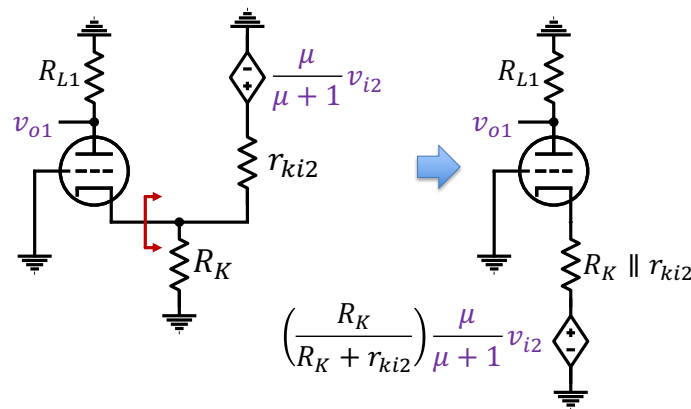


Figure 20. Replacing the portion of the right diagram of Figure 19 seen looking out of the cathode of the left tube with its Thévenin equivalent.

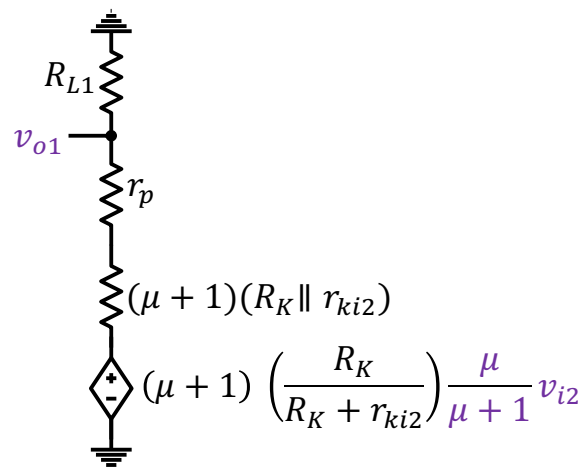


Figure 21. Replacing the portion of the right diagram of Figure 20 seen looking down into the plate with its Thévenin equivalent.

Using superposition, we combine (18) and (19) to yield

$$v_{o1} = \frac{\mu R_{L1}}{r_p + R_{L1} + (\mu + 1)(R_K \parallel r_{ki2})} \left(-v_{i1} + v_{i2} \frac{R_K}{R_K + r_{ki2}} \right). \tag{20}$$

Some designers let $R_{L1} = R_{L2}$, as seems natural; others set them to have different values in an attempt to compensate for the effect of the $R_K / (R_K + r_{ki2})$ factor.

Zeroing v_{i2} in Figure 21 yields the following output impedance:

$$r_{o1} = R_{L1} \parallel [r_p + (\mu + 1)(R_K \parallel r_{ki2})]. \tag{21}$$

The equivalent formulas for the second output can be derived from (17), (20), and (21) by swapping symbols:

$$r_{ki1} = \frac{r_p + R_{L1}}{\mu + 1}, \tag{22}$$

$$v_{o2} = \frac{\mu R_{L2}}{r_p + R_{L2} + (\mu + 1)(R_K \parallel r_{ki1})} \left(-v_{i2} + v_{i1} \frac{R_K}{R_K + r_{ki1}} \right), \tag{23}$$

$$r_{o2} = R_{L2} \parallel [r_p + (\mu + 1)(R_K \parallel r_{ki1})]. \tag{24}$$

For clarity, we assume that μ and r_p are the same for both tubes; one could study the effect of mismatched tubes by repeating the analysis with “1” and “2” subscripts on the small-signal parameters.

The direct derivation given above can be contrasted with the more cumbersome exposition on pp. 96–99 of [52], which involves solving a set of simultaneous equations.

4. Conclusions and Directions for Future Work

This paper presents Thévenin equivalent circuits looking into the positive and negative terminals of the VCVS of the small-signal triode model. The former corresponds to looking into the cathode, and the latter can be interpreted as looking into the plate side of the tube but bypassing the dynamic plate resistance (r_p), which can be readily added back in. We applied these equivalent circuits to the three standard single-tube amplifier configurations and a differential pair amplifier. The equivalent circuits let us intuitively derive gains, as well as input and output impedances, without having to solve systems of node-voltage or mesh-current equations. This approach can be applied to other structures, such as cascodes.

The title of Leach’s paper [35], which inspired this one, contained the words “and Signal Flow Graphs”, which are missing from the title of this paper. Leach used Mason flow graphs [56] to analyze transistor feedback amplifiers. Although some guitar amplifiers

use feedback from the speaker side of the output transformer of their power amplifier to help linearize the response, it is rare to find guitar amplifiers that use feedback in preamplifier stages, so we did not consider this case here. We conjecture that this is because the parameters of tubes are generally more consistent than those of transistors; in transistor circuits, feedback is a useful way of handling transistor variation. Future work could explore the analysis of feedback amplifiers using our Thévenin equivalent circuits combined with Mason flow graph techniques.

The analysis reported in this paper could be characterized as “midband”, since it assumes that capacitors can be approximated as short circuits for small signals. The Thévenin equivalent circuits presented in this paper could be readily extended from resistances to generic impedances and used to determine the effect of component capacitors and parasitic capacitances on the bass and treble responses.

This paper is dedicated in loving memory of Marshall Leach, who was always generous with his time and knowledge and was extremely patient with the author and his many questions.

Funding: This research received no external funding.

Data Availability Statement: No new data were created or analyzed in this study. Data sharing is not applicable to this article.

Conflicts of Interest: The author declares no conflict of interest.

Abbreviations

The following abbreviations are used in this manuscript:

BJT	Bipolar junction transistor
FET	Field-effect transistor
VCVS	Voltage-controlled voltage source

References

1. Hamm, R. Tubes Versus Transistors-Is There an Audible Difference. *J. Audio Eng. Soc.* **1973**, *21*, 267–273.
2. Leach, W. SPICE Models for Vacuum-Tube Amplifiers. *J. Audio Eng. Soc.* **1995**, *43*, 117–126.
3. Sjursen, W. Improved SPICE Model for Triode Vacuum Tubes. *J. Audio Eng. Soc.* **1997**, *45*, 1082–1088.
4. Kashuba, A. Ab Initio Model for Triode Tube. *J. Audio Eng. Soc.* **1999**, *47*, 373–377.
5. Tsambos, P. Three-Halves-Power Law Models for Actual Vacuum Tubes. *J. Audio Eng. Soc.* **2020**, *68*, 441–453. [[CrossRef](#)]
6. Oshimo, S.; Hamasaki, T. Physically Based Unified Modeling for a Series of Miniature Twin Triode Tubes. *J. Audio Eng. Soc.* **2018**, *66*, 808–822. [[CrossRef](#)]
7. Abuelma'atti, M. Large-Signal Analysis of Triode Vacuum-Tube Amplifiers. *J. Audio Eng. Soc.* **2003**, *51*, 1046–1053.
8. Orcioni, S.; Terenzi, A.; Cecchi, S.; Piazza, F.; Carini, A. Identification of Volterra Models of Tube Audio Devices using Multiple-Variance Method. *J. Audio Eng. Soc.* **2018**, *66*, 823–838. [[CrossRef](#)]
9. Pittman, A. *The Tube Amp Book*, Deluxe Revised ed.; Backbeat: London, UK, 2003.
10. Hunter, D. *The Guitar Amp Handbook: Understanding Tube Amplifiers and Getting Great Songs*; Backbeat: London, UK, 2005.
11. Hunter, D. *Guitar Rigs: Classic Guitar and Amp Combinations*; Backbeat: London, UK, 2005.
12. Barbour, E. The Cool Sound of Tubes. *IEEE Spectr.* **1998**, *35*, 24–35. [[CrossRef](#)]
13. Pakarinen, J.; Yeh, D. A Review of Digital Techniques for Modeling Vacuum-Tube Guitar Amplifiers. *Comput. Music J.* **2009**, *33*, 85–100. [[CrossRef](#)]
14. Neumann, U.; Irving, M. *Guitar Amplifier Overdrive: A Visual Tour*; Lulu: Raleigh, NC, USA, 2015.
15. Kuehnel, R. *Guitar Amplifier Electronics: System Design*; Amp Books: Seattle, WA, USA, 2019.
16. Kuehnel, R. *Guitar Amplifier Electronics: Circuit Simulation*; Amp Books: Seattle, WA, USA, 2019.
17. Kuehnel, R. *Guitar Amplifier Electronics: Fender Bassman*; Amp Books: Seattle, WA, USA, 2021.
18. Kuehnel, R. *Guitar Amplifier Electronics: Fender Deluxe*; Amp Books: Seattle, WA, USA, 2021.
19. Kuehnel, R. *Guitar Amplifier Electronics: Soldano SLO*; Amp Books: Seattle, WA, USA, 2021.
20. Hood, J. *Valve and Transistor Audio Amplifiers*; Newnes: Oxford, UK, 1997.
21. Jones, M. *Valve Amplifiers*, 3rd ed.; Newnes: Oxford, UK, 2003.
22. Jones, M. *Building Valve Amplifiers*; Newnes: Oxford, UK, 2004.
23. Rozenblit, B. *Tubes and Circuits*; Transcendent Sound: Kansas City, MO, USA, 2012.
24. *Circuits for Audio Amplifiers*; Segment: Vernon, CT, USA, 1959.

25. Tomasin, L.; Bevilacqua, A. A Time-Variant Analysis of Passive Resistive Mixers Using Thévenin Theorem. In Proceedings of the 2023 18th Conference on Ph.D Research in Microelectronics and Electronics (PRIME), Valencia, Spain, 18–21 June 2023. [CrossRef]
26. Zhou, X.; Liu, Y.; Chang, P.; Xue, F.; Zhang, T. Voltage Stability Analysis of a Power System with Wind Power Based on the Thévenin Equivalent Analytical Method. *Electronics* **2022**, *11*, 1758. [CrossRef]
27. Donnelly, T.; Pekarek, S.; Fudge, D.; Zarate, N. Thévenin Equivalent Circuits for Modeling Common-Mode Behavior in Power Electronic Systems. *IEEE Open Access J. Power Energy* **2020**, *7*, 163–172. [CrossRef]
28. Holder, M. Thévenin's Theorem and a Black Box. *IEEE Trans. Educ.* **2009**, *52*, 573–575. [CrossRef]
29. Su, H.Y.; Liu, T.Y. Robust Thévenin Equivalent Parameter Estimation for Voltage Stability Assessment. *IEEE Trans. Power Syst.* **2018**, *33*, 4637–4639. [CrossRef]
30. Sun, T.; Li, Z.; Rong, S.; Lu, J.; Li, W. Effect of Load Change on the Thévenin Equivalent Impedance of Power System. *Energies* **2017**, *10*, 330. [CrossRef]
31. Heydt, G. Thévenin's Theorem Applied to the Analysis of Polyphase Transmission Circuits. *IEEE Trans. Power Deliv.* **2017**, *32*, 72–77. [CrossRef]
32. Barletta, G.; DiPrima, P.; Papurello, D. Thévenin's Battery Model Parameter Estimation Based on Simulink. *Energies* **2022**, *15*, 6207. [CrossRef]
33. Salazar, D.; Garcia, M. Estimation and Comparison of SOC in Batteries Used in Electromobility Using the Thévenin Model and Coulomb Ampere Counting. *Energies* **2022**, *15*, 7204. [CrossRef]
34. Suti, A.; Di Rito, G.; Mattei, G. Development and Experimental Validation of Novel Thévenin-Based Hysteretic Models for Li-Po Battery Packs Employed in Fixed-Wing UAVs. *Energies* **2022**, *15*, 9249. [CrossRef]
35. Leach, W. On the Application of Thévenin and Norton Equivalent Circuits and Signal Flow Graphs to the Small-Signal Analysis of Active Circuits. *IEEE Trans. Circuits Syst.—I Fundam. Theory Appl.* **1996**, *43*, 885–893. [CrossRef]
36. Leach, W. On the Application of Superposition to Dependent Sources in Circuit Analysis. Available online: <https://leachlegacy.ece.gatech.edu/papers/superpos.pdf> (accessed on 25 November 2023).
37. Damper, R. Can Dependent Sources be Suppressed in Electrical Circuit Theory? *Int. J. Electron.* **2011**, *98*, 543–553. [CrossRef]
38. Davis, A. Some Fundamental Topics in Introductory Circuit Analysis: A Critique. *IEEE Trans. Educ.* **2000**, *43*, 330–335. [CrossRef]
39. Jaeger, R.; Blalock, T. *Microelectronic Circuit Design*, 4th ed.; McGraw-Hill Education: New York, NY, USA, 2010.
40. Sedra, A.; Smith, K.; Carusone, T.; Gaudet, V. *Microelectronic Circuits*, 8th ed.; Oxford University Press: Oxford, UK, 2019.
41. Leach, W. *Fundamentals of Low-Noise Electronics*, 4th ed.; Kendall Hunt: Dubuque, IA, USA, 2012.
42. Reich, H. *Principles of Electron Tubes*; McGraw-Hill: New York, NY, USA 1941.
43. Cruft Electronics Staff. *Electronic Circuits and Tubes*; McGraw-Hill: New York, NY, USA 1947.
44. Fischer, B. *Radio and Television Mathematics*; Macmillan: London, UK 1949.
45. DeFrance, J. *Electronic Tubes and Semiconductors*; Prentice-Hall: Hoboken, NJ, USA, 1958.
46. Kuehnel, R. *Guitar Amplifier Electronics: Basic Theory*; Amp Books: Seattle, WA, USA, 2018.
47. Kuehnel, R. *Vacuum Tube Circuit Design: Guitar Amplifier Preamps*, 2nd ed.; Amp Books: Seattle, WA, USA, 2009.
48. Hood, J. *Design and Construction of Tube Guitar Amplifiers*, 3rd ed.; TacTec Press: San Jose, CA, USA, 2012.
49. Brazee, J. *Semiconductor and Tube Electronics*; Holt, Rinehart and Winston: New York, NY, USA, 1968.
50. Blencowe, M. *Designing Tube Preamps for Guitar and Bass*; Lulu: Raleigh, NC, USA, 2009.
51. Dailey, D. *Electronics for Guitarists*, 2nd ed.; Springer: New York, NY, USA, 2013.
52. Kuehnel, R. *Circuit Analysis of a Legendary Tube Amplifier: The Fender Bassman 5F6-A*, 3rd ed.; Amp Books: Seattle, WA, USA, 2009.
53. Everitt, W., Ed. *Fundamentals of Radio and Electronics*, 2nd ed.; Prentice Hall: Seattle, WA, USA, 1958.
54. Millman, J. *Vacuum-Tube and Semiconductor Electronics*; McGraw-Hill: New York, NY, USA 1958.
55. Kuehnel, R. *Vacuum Tube Circuit Design: Guitar Amplifier Power Amps*, 2nd ed.; Amp Books: Seattle, WA, USA, 2008.
56. Mason, S. Feedback Theory—Further Properties of Signal Flow Graphs. *Proc. IRE* **1956**, *44*, 920–296. [CrossRef]

Disclaimer/Publisher's Note: The statements, opinions and data contained in all publications are solely those of the individual author(s) and contributor(s) and not of MDPI and/or the editor(s). MDPI and/or the editor(s) disclaim responsibility for any injury to people or property resulting from any ideas, methods, instructions or products referred to in the content.